Grzegorz SZERSZEŃ[1], Franciszek WITOS[2]

18. APPLICATION OF SELECTED ACOUSTIC EMISSION DESCRIPTORS TO IDENTIFY PARTIAL DISCHARGE

18.1. Introduction

Acoustic Emission Signal (AE) analysis can be performed in many areas. The basic domains are time, frequency, time-frequency and threshold of discrimination. The description of the analyzed signals is carried out using descriptors.

Acoustic emission (AE) is understood either as a physical phenomenon or as a research method. In the physical phenomenon, the process of generating AE elastic waves and the description of the form of these waves at any point in the material as a function of time is important, while in the measurement method, it is important to record the AE elastic waves and their analysis. The elements of AE understood as a measurement and research method are measuring apparatus and methods of data analysis.

The physical phenomenon of AE consists in the fact that during the deformation processes a local remodeling of the structure of the medium takes place, during which some of the accumulated energy may be emitted in the form of AE pulses. The generated AE pulses propagate in the medium and, by means of AE sensors, are recorded as signals, which are then analyzed. Recorded signals can be of two types, pulse or continuous.

The paper presents analyzes of AE signals from partial discharges (PD) generated by a specially modeled PD source. A high AC voltage of 50 Hz was applied to the modeled PD source. Due to the complex processes that occur during the initiation and maintenance of the examined PDs, the PD signals are very complex. The complicated nature of the signals makes it necessary to take into account the stochasticity of the phenomenon. Each measurement test included the registration of the signal for about 100 periods of alternating voltage (single measurements lasted two seconds each) and then the analysis of the properties of the recorded

[1] Department of Electronics and Telecommunications, Polytechnic Faculty, University of Applied Sciences in Tarnow, ul. Mickiewicza 8, 33-100 Tarnow, Poland, g_szerszen@pwsztar.edu.pl
[2] Department of Optoelectronics, Faculty of Electrical Engineering, Silesian University of Technology, ul. Krzywoustego 2, 44-100 Gliwice, Poland, franciszek.witos@polsl.pl

signal was carried out. The most important element of the work is the analysis of the descriptors of the recorded AE signals in the field of the discrimination threshold [6].

18.2. Investigations of partial discharges in systems with a modeled source

18.2.1. Description of the measuring station

Investigations of PDs coming from a modeled source were performed in parallel by two methods: the AE method – with the use of the constructed measuring system 8AE-PD and the electrical method with the use of the PD measuring system of type TE 571 produced by Haefely Trench Tettex Instruments [1, 3]. The investigation results obtained from the electrical method, particularly the measurement of the apparent charge introduced by the PD source are the reference for the results from the acoustic emission metod [2]. In [6], such a methodology is named as the calibrated acoustic emission. The investigations were carried out on the measurement stand whose schematic diagram is shown in Fig. 1. This stand includes: a test set generating high voltage (with a protection and regulation system), the computer PD measuring system with TE 571 measuring instrument and additional equipment, a steel tank in the form of a cuboid with dimensions of 58×110×60 cm (width×length×height), a modeled PD source and the measuring system 8AE-PD. Laboratory tests were carried out with the use of various models of PD sources and for the sake of order they were called subsequent letters of the alphabet.

Type B source is the result of searching for a more complex measurement object with stable PD. It was made of a rectangular textolite with a hollow hole, filled with steel filings and closed with resin (Fig. 2). On the opposite sides of the cuboid there are flat electrodes connected to high voltage and to ground. The arrangement of elements inside the tank for this structure is presented in Fig. 2b. Measurements were made for various model settings in relation to sensors (configurations K3 - K6). This way, the optimal setting for which the level of recorded AE signals was the highest was searched for. In this type of sources, large electrode surfaces applied to the prepared cuboid in a hollow hole make it difficult to propagate AE elastic waves in the direction of the electrode axis [4].

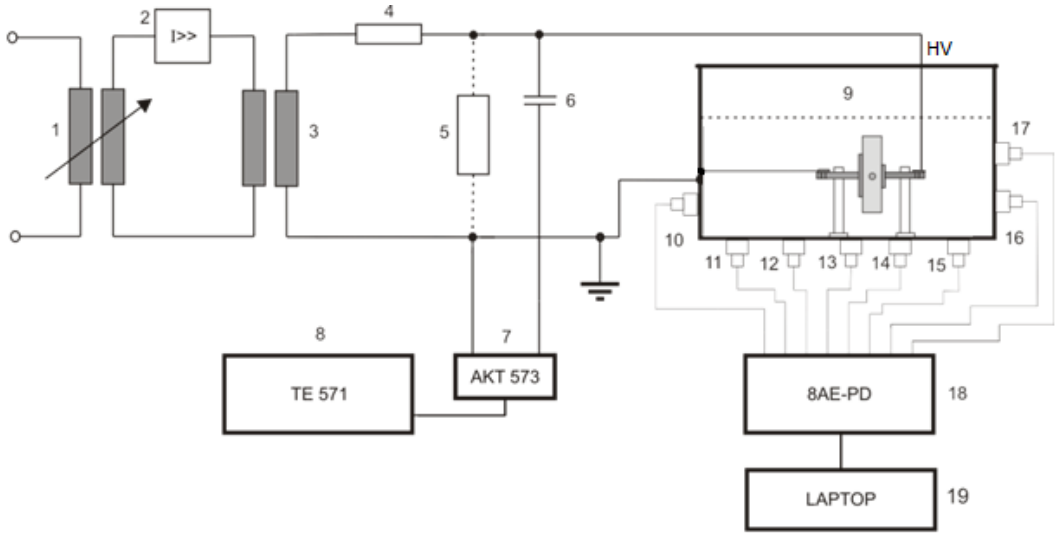

Fig. 1. Schematic diagram of the system for generating and testing PDs by the electrical and acoustic methods: 1 – autotransformer, 2 – overcurrent protection, 3 – high voltage transformer, 4 – protective resistance, 5 – calibrator KAL 451, 6 – coupling capacitor, 7 – coupling four-terminal network AKT 573, 8 – TE571 system, 9 – tank with the PD source, 10-17 – AE sensors, 18 – measuring system 8AE-PD, 19 – recording computer

Rys. 1. Schemat układu do generacji i badania WNZ metodą elektryczną i akustyczną: 1 – autotransformator, 2 – zabezpieczenie nadprądowe, 3 – transformator wysokiego napięcia, 4 – rezystancja ochronna, 5 – kalibrator KAL 451, 6 – kondensator sprzęgający, 7 – czwórnik sprzęgający AKT 573, 8 – system TE571, 9 – kadź ze źródłem WNZ, 10-17 – czujniki EA, 18 – system badawczy 8EA-WNZ, 19 – komputer rejestrujący

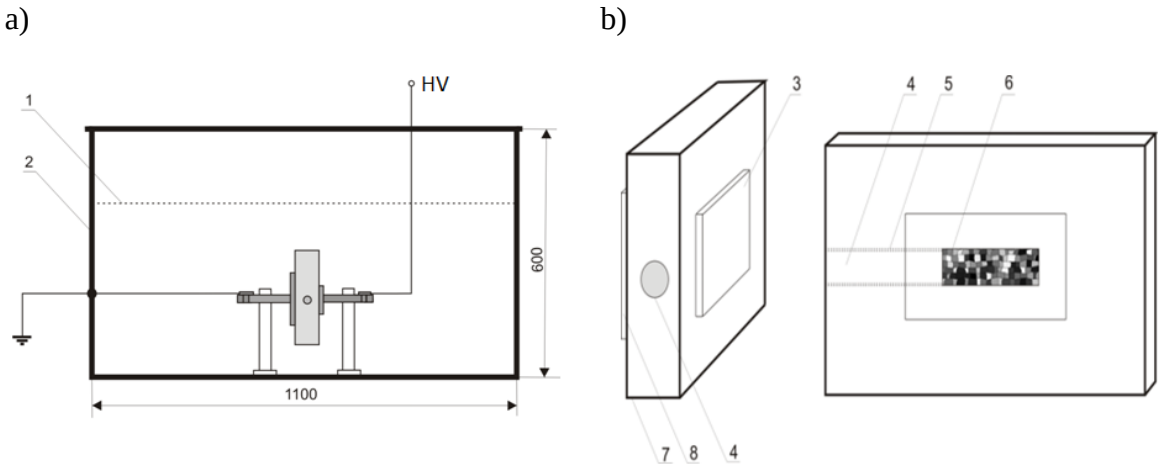

Fig. 2. Measuring tank with modeled PD source type B − a), modeled PD source type B − b); 1 − level of tranformer oil, 2 − steel tank, 3 − HV electrode, 4 − textilite stopper, 5 − layer of resin, 6 − chamber filled with steel filings, 7 − textolite plate, 8 − ground electrode

Rys. 2. Schemat kadzi ze źródłem typu B − a), zamodelowane źródło typu B − b); 1 – poziom oleju transformatorowego, 2 – stalowa kadź, 3 – elektroda wysokiego napięcia WN, 4 – korek tekstolitowy, 5 – warstwa żywicy, 6 – komora wypełniona stalowymi opiłkami, 7 – płyta tekstolitu, 8 – elektroda uziemienia

The tests were carried out using measurement configurations determined by the source type, positioning the source inside the measuring tank and the arrangement of AE sensors on the walls of the measuring tank [8]. The AE sensors were placed at selected points on the outside wall of the tank (Fig. 3) using magnetic holders. A coupling layer of technical vaseline provided the acoustic contact.

18.2.2. Selected measuring situations

For each configuration, the source setting and the location of the AE sensors were constant. The following four configurations were used in the research:

K3 - B type source transversely mounted inside the tank as shown in Fig. 3, AE sensors placed symmetrically, two on each wall.

K4 - B type source mounted transversely inside the tank, closer to one of the walls, as shown in Fig. 4, AE sensors placed in one plane.

K5 - B type source mounted transversely as shown in Fig. 5, blocked internal hole directed towards the bottom of the tank, AE sensors positioned as in the K4 configuration.

K6 - B type source mounted as in the K5 configuration, AE sensors No. 7 and 6 mounted on the bottom of the vat (Fig. 6) in line with sensors No. 0, 1 and 2.

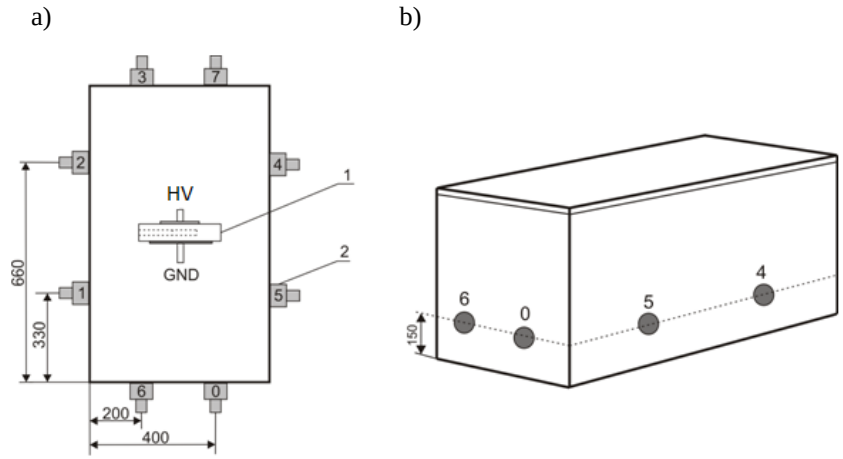

Fig. 3. Arrangement of AE sensors on the walls of the tank filled with transformer oil, K3 configuration, coordinates of the sensors are given in mm - a) top view, b) side view showing the location of AE sensors No. 0 - 7 on the side walls; 1 - B type source as the modeled PD source, 2 - measurement sensor No. 5 according to Table 1

Rys. 3. Rozmieszczenie czujników EA na ścianach kadzi wypełnionej olejem transformatorowym, konfiguracja K3, współrzędne czujników podano w mm: a) widok z góry, b) widok z boku z zaznaczeniem położenia czujników nr 0-7, 1 - obiekt B jako źródło WNZ, 2 - czujnik pomiarowy nr 5 wg tabeli 1

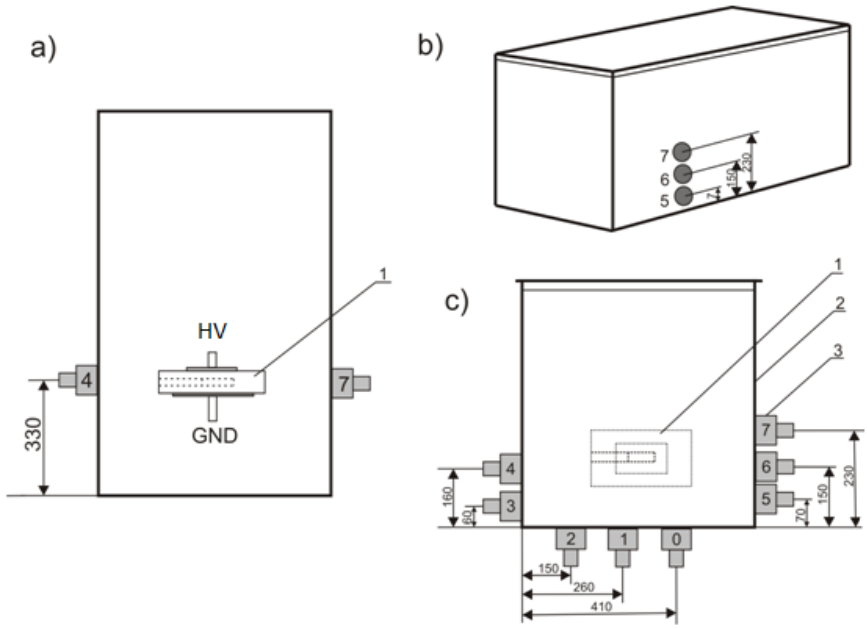

Fig. 4. Arrangement of AE sensors on the walls of the tank filled with transformer oil, K4 configuration, coordinates of the sensors are given in mm: a) top view, b) and c) side view with the location of AE sensors No. 0 - 7 on the side walls; 1 - object B as a PD source, 2 - tank, 3 - sensor No. 7 according to Table 1

Rys. 4. Rozmieszczenie czujników EA na ścianach kadzi wypełnionej olejem transformatorowym, konfiguracja K4, współrzędne czujników podano w mm: a) widok z góry, b) widok z boku z zaznaczeniem położenia czujników nr 0-7, 1 - obiekt B jako źródło WNZ, 2 - kadź, 3 - czujnik pomiarowy nr 7 wg tabeli 1

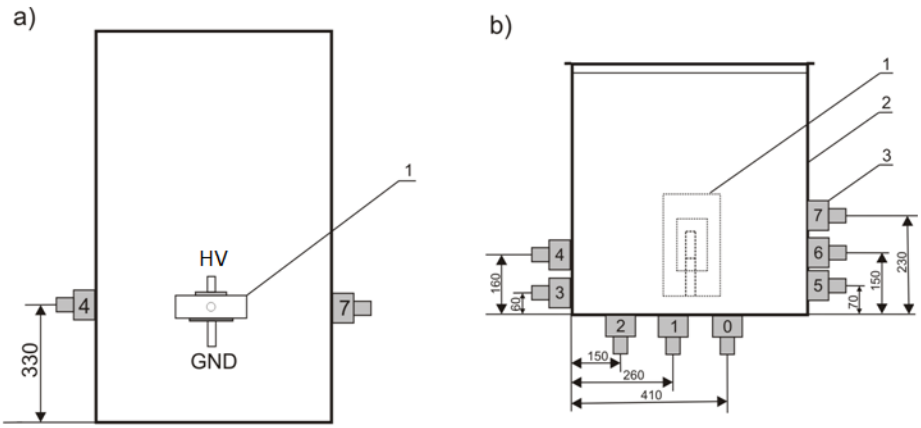

Fig. 5. Arrangement of AE sensors on the walls of the tank filled with transformer oil, K5 configuration, coordinates of the sensors are given in mm: a) top view, b) and c) side view with the location of AE sensors No. 0 - 7 on the side walls; 1 - object B in a vertical position as a PD source, 2 - tank, 3 - sensor No. 7 according to Table 1

Rys. 5. Rozmieszczenie czujników EA na ścianach kadzi wypełnionej olejem transformatorowym, konfiguracja K5, współrzędne czujników podano w mm: a) widok z góry, b) widok z boku z zaznaczeniem położenia czujników nr 0-7, 1 - obiekt B jako źródło WNZ, 2 - kadź, 3 - czujnik pomiarowy nr 7 wg tabeli 1

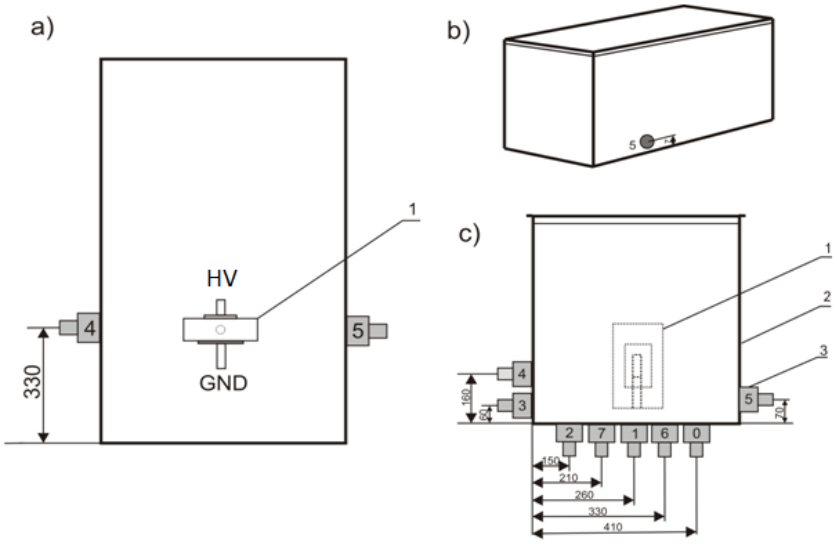

Fig. 6. Arrangement of AE sensors on the walls of the tank filled with transformer oil, K6 configuration, coordinates of the sensors are given in mm: a) top view, b) and c) side view with the location of AE sensors No. 0 - 7 on the side walls; 1 - object B as a PD source, 2 - tank, 3 - sensor No. 5 according to Table 1

Rys. 6. Rozmieszczenie czujników EA na ścianach kadzi wypełnionej olejem transformatorowym, konfiguracja K6, współrzędne czujników podano w mm: a) widok z góry, b) i c) widok z boku z zaznaczeniem położenia czujników nr 0-7, 1 - obiekt B jako źródło WNZ, 2 - kadź, 3 - czujnik pomiarowy nr 5 wg tabeli 1

Table 1

Connection of measuring lines of the 8AE-PD system with measuring sensors [8]

Designation of the measuring sensor in the diagrams	Name of the measurement path in the 8AE-PD system	Measurement sensor type	Additional devices
0	CH0	D 9241A – J88, dual BNC	Preamplifier **
1	CH1	D 9241A – J89, dual BNC	Preamplifier **
2	CH2	D 9241A – J90, dual BNC	Preamplifier **
3	CH3	D 9241A – J91, dual BNC	Preamplifier **
4	CH4	D 9241A – J92, dual BNC	Preamplifier **
5	CH5	D 9241A – J102, dual BNC	Preamplifier **
6	CH6	WD, wideband, BNC	Preamplifier **
7	CH7	WDI, wideband 100 kHz – 1MHz, BNC	Without preamplifier
* preamplifier and sensor connected by a double coaxial cable terminated with two BNC plugs ** preamplifiers dedicated to the 8AE-PD system			

18.3. Quantitative analysis of PD signals from PD generated by B type sources in the 30 - 200 kilohertz band

The PD source named object B and described in subsection 2.1, was used in four measurement configurations named K3, K4, K5 and K6. The structure of the facility is shown in Fig. 2b. The conducted tests were aimed at checking the capabilities of the 8AE-PD measurement system in the location of complex PD sources with a small apparent charge and a small amplitude of AE signals reaching the sensors [10]. Tables 2 and 3 show the calculated values of ADP and ADC descriptors determined for signals recorded in eight measurement paths from CH0 to CH7 at a constant gain of 55 dB (K3, K4, K5) and in Table 4 for a gain of 46.8 dB (K6).

Table 2

List of measurement conditions and values of ADP and ADC descriptors in K3, configurations at 55 dB gain

Configuration	Collection name	Measurement path CH	*U*	*Q*	*I*	*N*	ADP	σ_{ADP}	ADC	σ_{ADC}
			kV	pC	nA	1/s	a.u.	a.u.	a.u.	a.u.
1	2	3	4	5	6	7	8	9	10	11
K3	M5_55 dB	0	19.3	200	35	300	-7695.1	2616.8	-8525.9	2248.9
		1					-8794.6	1224.0	-9651.9	901.7
		2					-8514.1	3478.9	-9506.0	3131.2
		3					-7658.0	2368.7	-8469.9	2017.5
		4					-9127.7	1162.5	-9933.5	829.3
		5					-8516.3	810.4	-9395.9	677.0
		6					-9242.9	4390.7	-10309.9	4347.3
		7					-14436.4	699.5	-15416.3	754.5
K3	M_55dB noise	0	0	0	0	0	-9656.5	237.9	-10346.7	335.5
		1					-9883.0	429.9	-10642.2	428.8
		2					-10287.9	495.4	-11033.6	502.0
		3					-9801.9	256.1	-10476.0	125.2
		4					-9609.3	275.7	-10293.3	210.7
		5					-9236.0	193.7	-10050.1	247.5
		6					-11723.3	219.7	-12743.9	273.4
		7					-15100.6	1168.1	-15973.6	985.0

In the K3 configuration, the calculated values of ADC and ADP descriptors (Table 2) indicate a noticeable degree of advancement of AE signals, hence it can be concluded that they come from a working PD source. Their values are greater than those determined for the set recorded as noise (M_55dBnoise). The analysis of signals in the time domain in this case is very difficult, as illustrated in Fig. 7 - 9, and drawing conclusions as to the presence of a PD source is uncertain. The symmetrical arrangement of the sensors (Fig. 3) on the walls of the tank allows you to compare the results obtained for the same type of sensors (lines CH0 to

CH5). The differences in the descriptor values, entered in column 8 and 10 of Table 2, may be due to the complicated mechanism of AE signals propagation inside the vat, due to multiple reflections and interferences. Significantly different levels of ADP and ADC descriptors were obtained in the CH7 path, but this is due to different parameters of this sensor, mainly the passband.

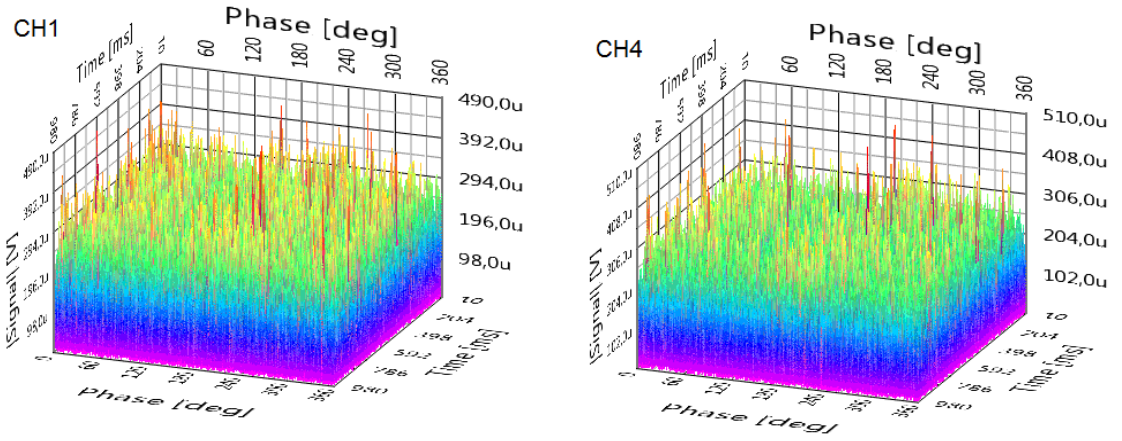

Fig. 7. Phase-time characteristics of signals recorded in measurement channels CH1 and CH4 in the K3 configuration for the data set M5_55dB

Rys. 7. Charakterystyki fazowo-czasowe sygnałów zarejestrowanych w torach pomiarowych CH1 i CH4 w konfiguracji K3 dla zbioru danych M5_55dB

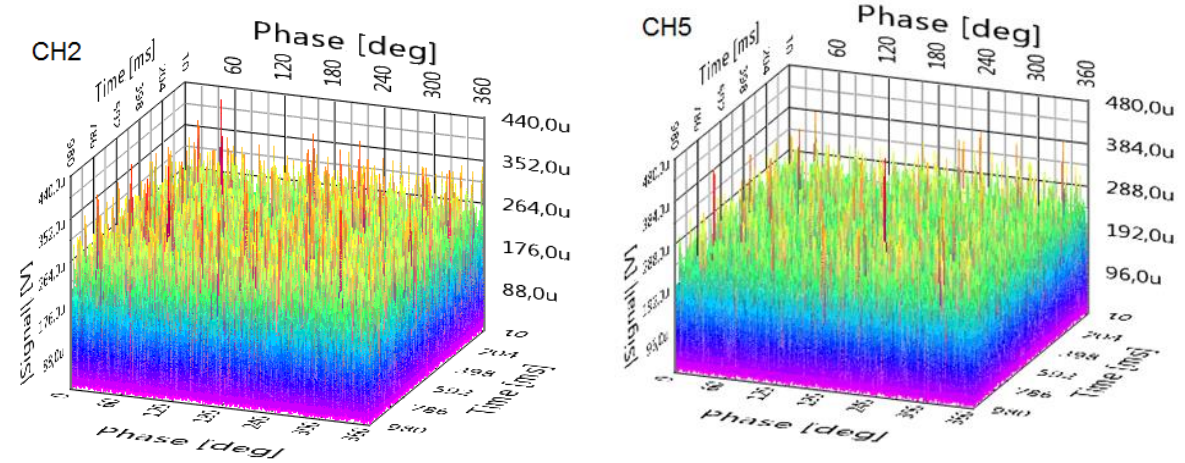

Fig. 8. Phase-time characteristics of signals recorded in measurement channels CH2 and CH5 in the K3 configuration for the data set M5_55dB

Rys. 8. Charakterystyki fazowo-czasowe sygnałów zarejestrowanych w torach pomiarowych CH2 i CH5 w konfiguracji K3 dla zbioru danych M5_55dB

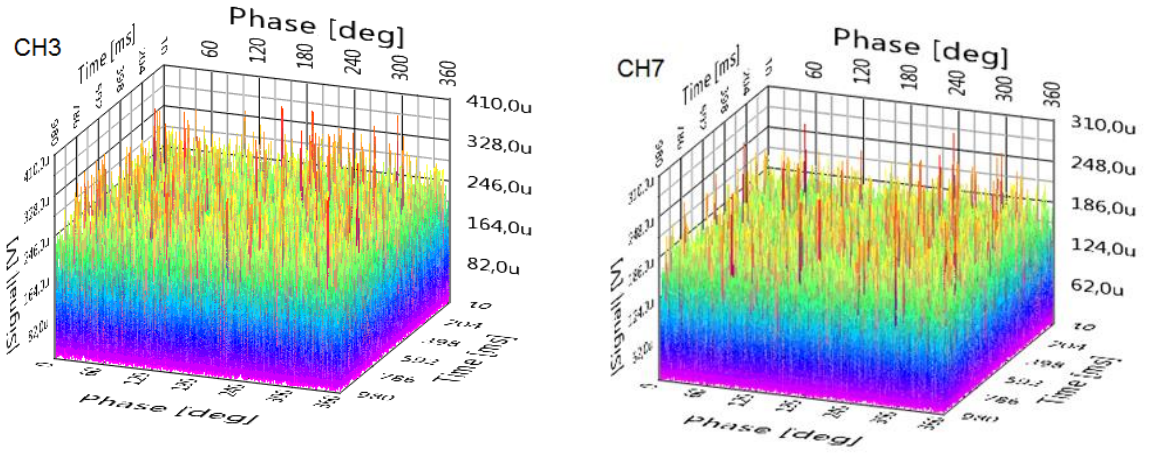

Fig. 9. Phase-time characteristics of signals recorded in measurement channels CH3 and CH7 in the K3 configuration for the data set M5_55dB

Rys. 9. Charakterystyki fazowo-czasowe sygnałów zarejestrowanych w torach pomiarowych CH3 i CH7 w konfiguracji K3 dla zbioru danych M5_55dB

The change in the location of the measuring sensors in relation to the source in the K4 configuration (Fig. 10) caused that the descriptor values calculated for the signals recorded with he sensors located closest to the PD source increased significantly (Table 3).

Table 3

Measurement conditions and values of ADP and ADC descriptors in K4 and K5 configurations at 55 dB gain

Configuration	Collection name	Measurement pathCH	U	Q	I	N	ADP	σ_{ADP}	ADC	σ_{ADC}
			kV	pC	nA	1/s	a.u.	a.u.	a.u.	a.u.
1.	2.	3.	4.	5.	6.	7.	8.	9.	10.	11.
K4	M11_55 dB	0	19.8	300	55	300	-6184.4	497.8	-7065.8	463.6
		1					-6182.8	598.6	-7865.6	506.0
		2					-6206.1	870.2	-7457.1	606.9
		3					-4036.2	512.0	-5239.5	568.4
		4					-7043.1	1318.9	-7278.3	623.0
		5					-242857.9	11034.2	-262833.9	11210.8
		6					-15236.3	679.2	-16224.7	717.1
		7					-10472.4	717.8	-11668.8	381.4
K5	M21_55 dB	0	19.8	400	55	300	-1322.6	816.1	-1940.3	953.0
		1					-1286.0	579.7	-1652.3	744.2
		2					-2070.0	1028.2	-2959.9	1035.5
		3					-1364.0	705.9	-2004.8	812.7
		4					-1745.8	1181.5	-2944.4	1487.7
		5					-240841.9	11438.0	-262098.0	13230.3
		6					-13753.3	1465.2	-15497.0	723.9
		7					-478.5	366.3	-1029.9	675.0

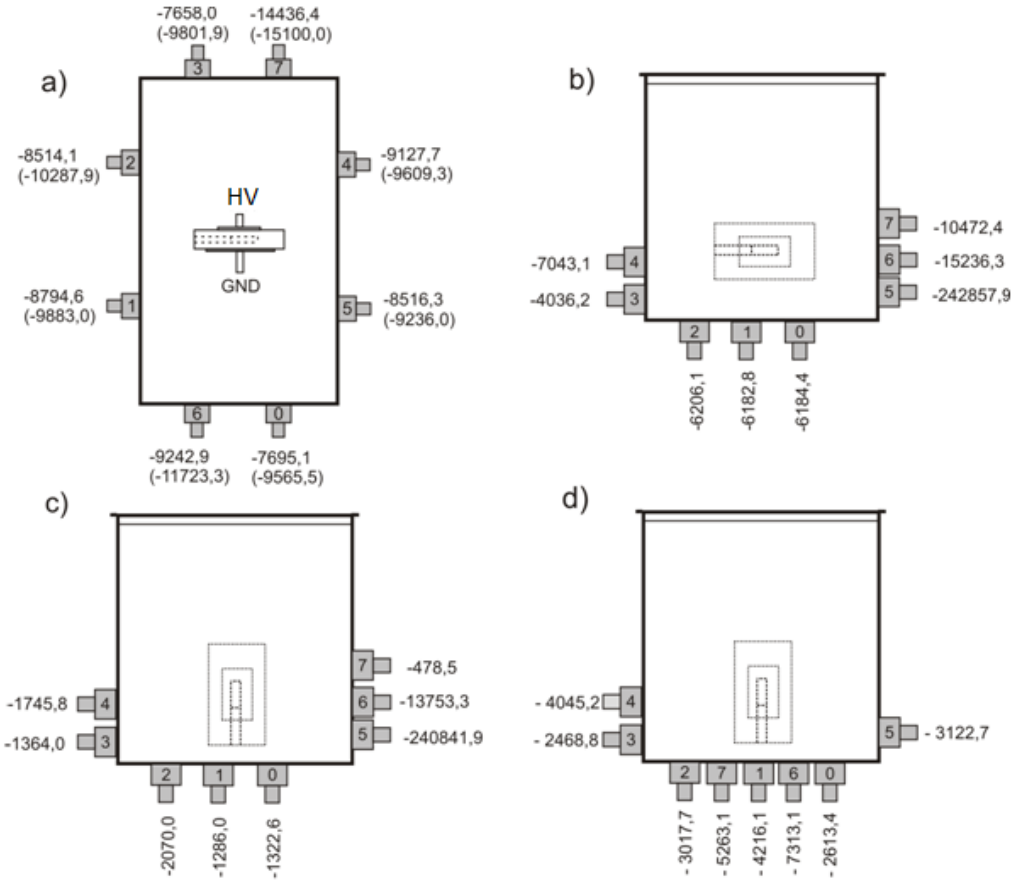

Fig. 10. Distribution of ADP descriptors values in the following measurement situations: a) K3 configuration, 55 dB, 19.3 kV, 200 pC, descriptor values in parentheses corresponding to noise (M_55dB_noise set), b) K4.55 dB configuration, 19.8 kV, 300 pC, c) K5 configuration, 55 dB, 19.8 kV, 400 kV, d) K6 configuration, 46.8 dB, 19.8 kV, 400 pC (M23_46.8dB set)

Rys. 10. Rozkład wartości deskryptorów ADP w następujących sytuacjach pomiarowych: a) konfiguracja K3, 55 dB, 19,3 kV, 200 pC, wartości deskryptorów w nawiasach odpowiadające szumowi (zestaw M_55dB_szum), b) konfiguracja K4,55 dB, 19,8 kV, 300 pC, c) konfiguracja K5, 55 dB, 19,8 kV, 400 kV, d) konfiguracja K6, 46,8 dB, 19,8 kV, 400 pC (zestaw M23_46,8dB)

Within K4 configuration the apparent charge *Q* was increased to 300 pC, slightly increasing the test voltage *U* to 19.8 kV. Especially in the CH1, CH3 and CH4 paths, the values of ADP and ADC descriptors increased compared to the K3 configuration (Fig. 11 - 13).

The obtained results are confirmed by the shapes of the phase-time characteristics (Fig. 14a) and characteristic changes in the amplitude as a function of the phase on the averaged STFT spectrogram (Fig. 14b). The obtained results indicate the presence of signals from PD sources. Due to the frequency band of the PDs generated and the location of the PD source, the broadband sensors on the CH6 and CH7 lines did not register any useful AE signals.

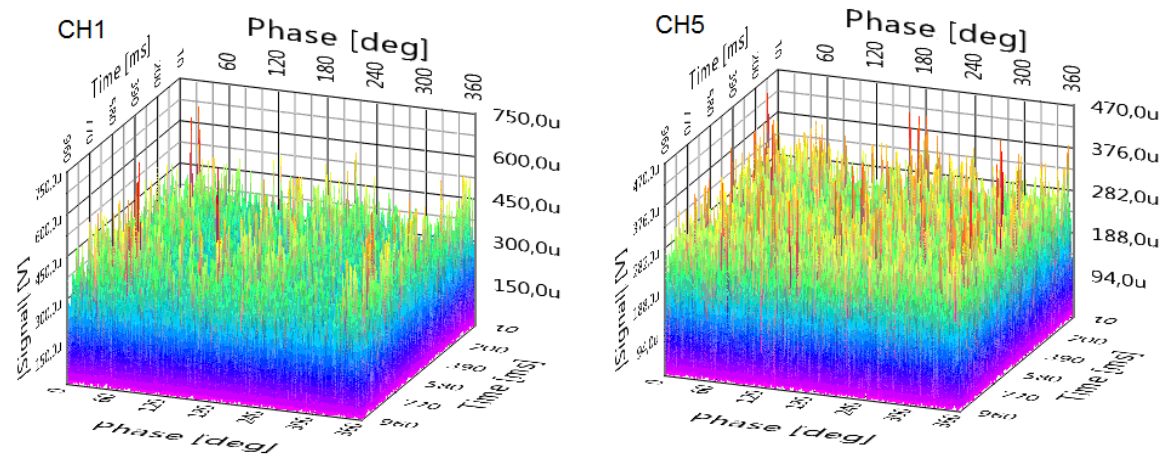

Fig. 11. Phase-time characteristics of signals recorded in measurement channels CH1 and CH5 in the K4 configuration for the M11_55dB data set

Rys. 11. Charakterystyki fazowo-czasowe sygnałów zarejestrowanych w torach pomiarowych CH1 i CH5 w konfiguracji K4 dla zbioru danych M11_55dB

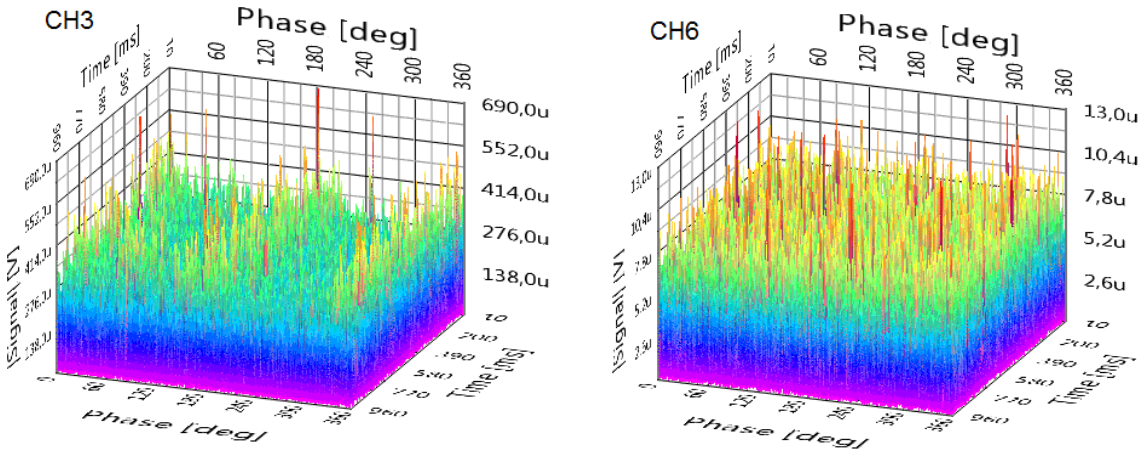

Fig. 12. Phase-time characteristics of signals recorded in measurement channels CH3 and CH6 in the K4 configuration for the M11_55dB data set

Rys. 12. Charakterystyki fazowo-czasowe sygnałów zarejestrowanych w torach pomiarowych CH3 i CH6 w konfiguracji K4 dla zbioru danych M11_55dB

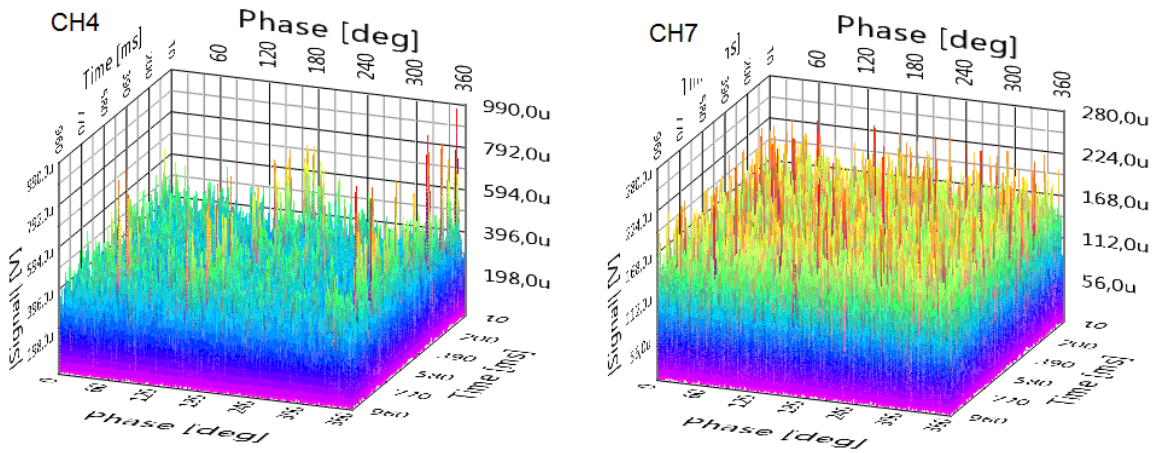

Fig. 13. Phase-time characteristics of signals recorded in measurement channels CH4 and CH7 in the K4 configuration for the M11_55dB data set

Rys. 13. Charakterystyki fazowo-czasowe sygnałów zarejestrowanych w torach pomiarowych CH4 i CH7 w konfiguracji K4 dla zbioru danych M11_55dB

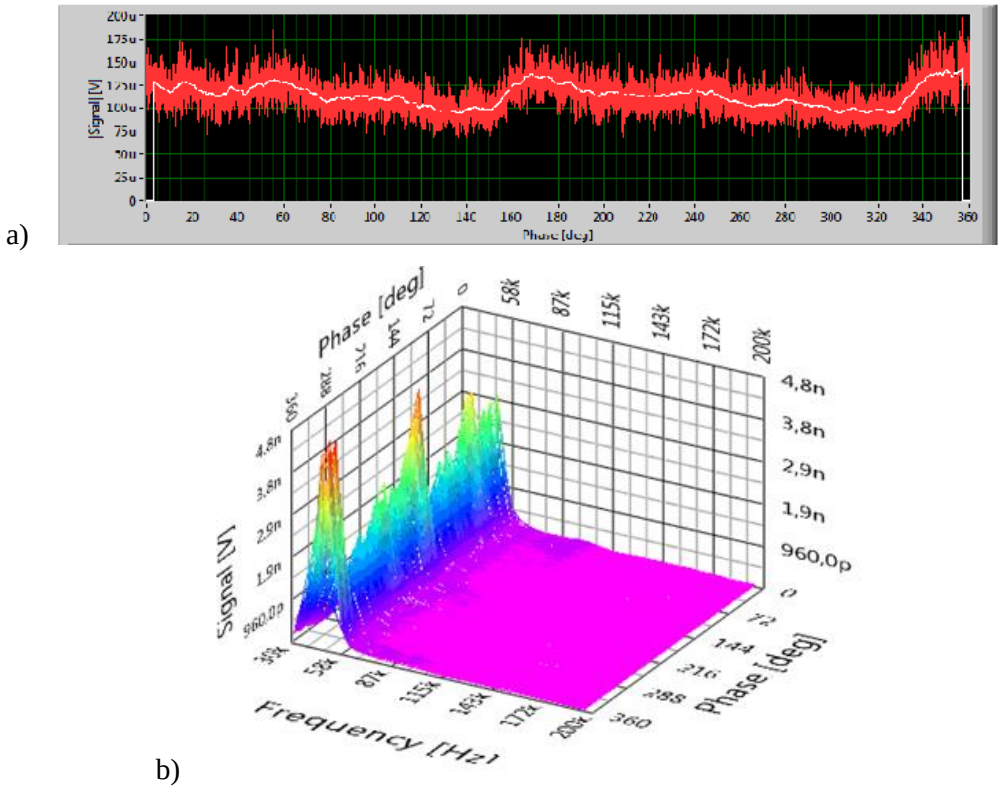

Fig. 14. AE signal recorded in the K4 configuration for the M11_55dB set in the CH3 measurement channel: a) averaged phase characteristic, b) averaged STFT spectrogram

Rys. 14. Sygnał AE zarejestrowany w konfiguracji K4 dla zestawu M11_55dB w torze pomiarowym CH3: a) uśredniona charakterystyka fazowa, b) uśredniony spektrogram STFT

In the next K5 configuration (Fig. 10c), the location of the PD source was changed, with the sensors positions unchanged, only improving the quality of the coupling layer by applying a new layer of technical petroleum jelly to the sensor heads (Fig. 5). The obtained descriptor values entered in column 8 and 10 of Table 3, indicate their high degree of advancement, which is caused by the presence of AE signals from PD.

Fig. 15 - 17 shows the phase-time characteristics, the shape of which confirms the presence of PD. Due to the change in the location of the PD source, the AE signals with much larger amplitudes compared to the K4 configuration were recorded in the CH1, CH3 and CH4 lines (Fig. 11-13).

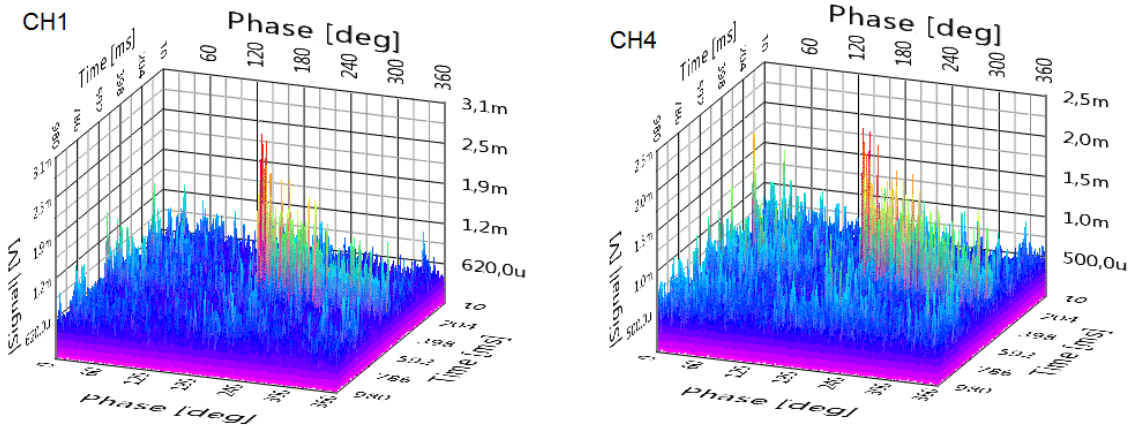

Fig. 15. Phase-time characteristics of signals recorded in measurement channels CH1 and CH 4 in the K5 configuration for the M21_55dB set

Rys. 15. Charakterystyki fazowo-czasowe sygnałów rejestrowanych w torach pomiarowych CH1 i CH4 w konfiguracji K5 dla zestawu M21_55dB

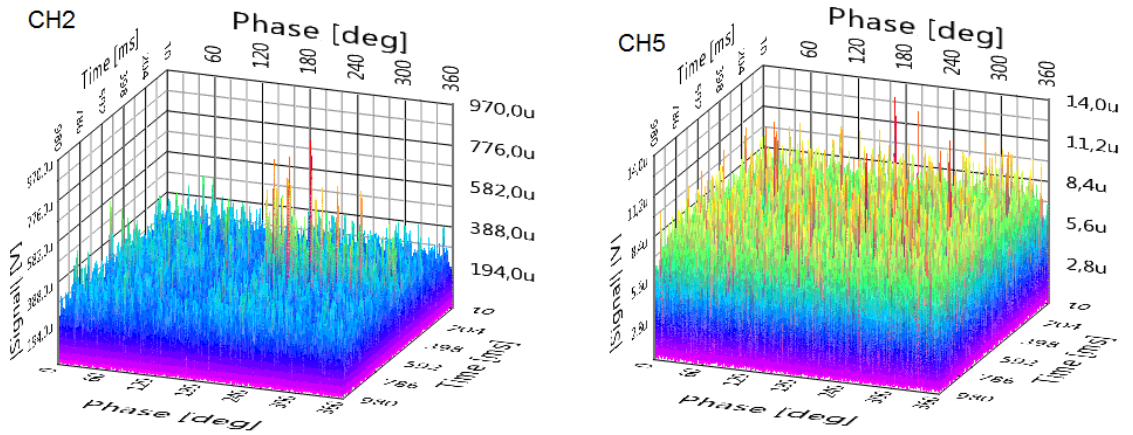

Fig. 16. Phase-time characteristics of signals recorded in measurement channels CH2 and CH5 in the K5 configuration for the M21_55dB set

Rys. 16. Charakterystyki fazowo-czasowe sygnałów rejestrowanych w torach pomiarowych CH2 i CH5 w konfiguracji K5 dla zestawu M21_55dB

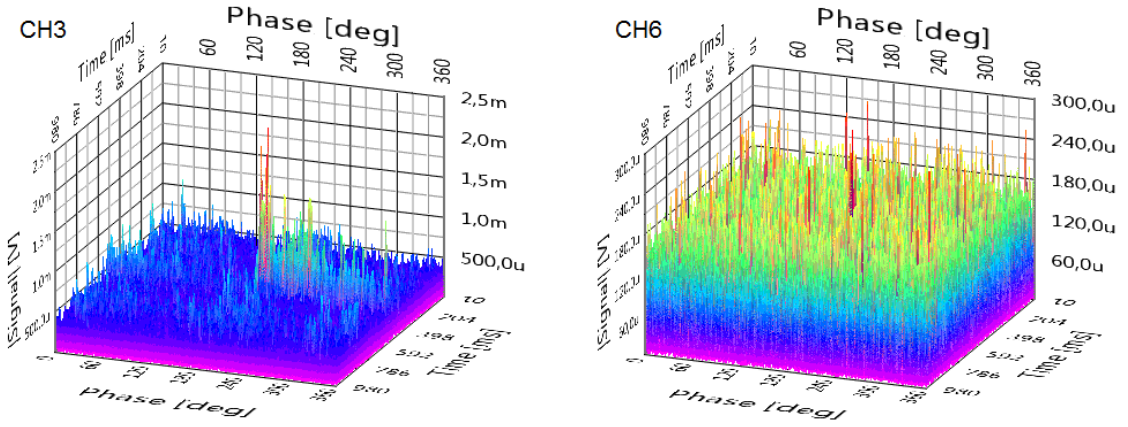

Fig. 17. Phase-time characteristics of signals recorded in measurement channels CH3 and CH6 in the K5 configuration for the M21_55dB set

Rys. 17. Charakterystyki fazowo-czasowe sygnałów rejestrowanych w torach pomiarowych CH3 i CH6 w konfiguracji K5 dla zestawu M21_55dB

AE signals were recorded in the CH7 channel by means of a broadband sensor, which can be associated with the presence of the PD source (Fig. 18 - 20). The signal was subjected to additional filtration in the 30 kHz - 200 kHz band.

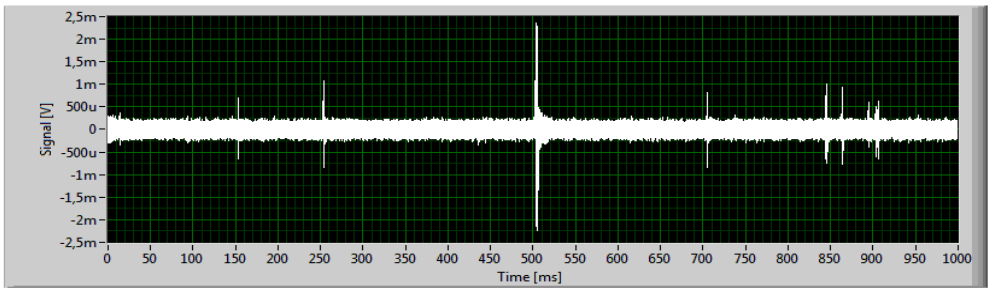

Fig. 18. AE signal recorded in the K5 configuration for the M21_55dB set in the CH7 measurement channel , signal after filtration in the 30 kHz - 200 kHz band

Rys. 18. Sygnał AE zarejestrowany w konfiguracji K5 dla zestawu M21_55dB w torze pomiarowym CH7, sygnał po filtracji w paśmie 30 kHz - 200 kHz

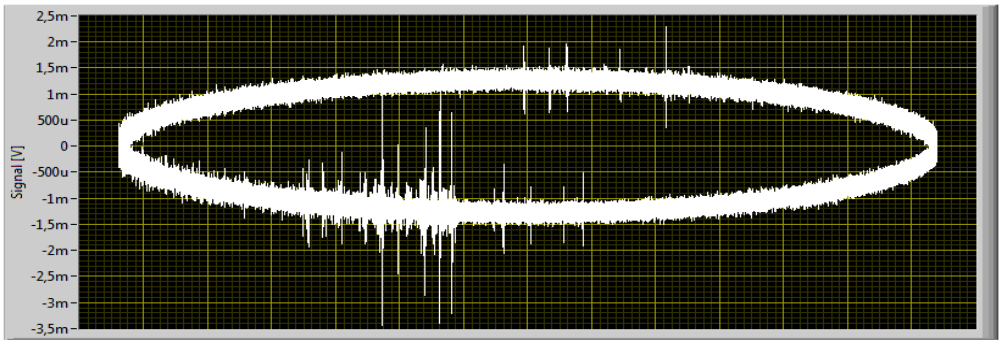

Fig. 19. AE signal recorded in the K5 configuration for the M21_55dB set in the CH7 measurement channel , phase characteristics
Rys. 19. Sygnał AE zarejestrowany w konfiguracji K5 dla zestawu M21_55dB w torze pomiarowym CH7, charakterystyka fazowa

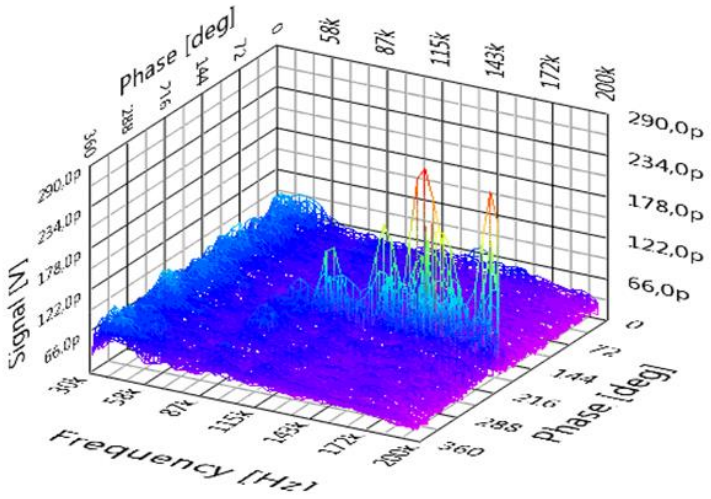

Fig. 20. AE signal recorded in the K5 configuration for the M21_55dB set in the CH7 measurement channel , averaged STFT spectrogram
Rys. 20. Sygnał AE zarejestrowany w konfiguracji K5 dla zestawu M21_55dB w torze pomiarowym CH7, uśredniony spektrogram STFT

In the K6 configuration, modifications were introduced to bring broadband sensors closer to the potential PD source (Fig. 6). Table 4 presents the results of calculations of ADP and ADC descriptors for four selected measurement situations, in which the gain remained constant at 46.8 dB, and the test voltage has been changed, thus the apparent charge value were changed from 0 to 400 pC. For the value of 100 pC and 200 pC involved by modeled PD source the descriptor values are close to those obtained for the noise signal. In the case of the M23_46.8dB set, in the presence of a relatively large apparent charge of 400 pC, the calculated values of the ADP and ADC descriptors confirm the presence of PD (columns 7 and 9 in Table 4).

Table 4

Summary of measurement conditions and values of ADP and ADC descriptors in K6 configuration for 46.8 dB gain

Collection name	MAEsurement pathCH	U	Q	I	N	ADP	σ_{ADP}	ADC	σ_{ADC}
		kV	pC	nA	1/s	a.u.	a.u.	a.u.	a.u.
1	2	3	4	5	6	7	8	9	10
M23_4 6.8dB	0	19.8	400	55	300	-2613.4	124.2	-2962.2	83.25
	1					-4216.1	109.75	-4549.3	171.05
	2					-3017.7	187.35	-3437.6	147.4
	3					-2468.8	220.8	-2928.8	100.5
	4					-4045.2	64.2	-4495.9	82.7
	5					-3122.7	182.2	-3482.6	137.1
	6					-7313.1	265.5	-7873.9	315.7
	7					-5263.1	494.1	-5905.3	338.7
M27_4 6.8dB	0	15.8	200	40	170	-8637.0	161.2	-9336.8	168.9
	1					-9497.3	316.7	-10107.6	348.7
	2					-9379.6	341.8	-9964.6	209.9
	6					-14310.0	410.2	-15297.5	370.1
	7					-11482.6	499.3	-12387.1	520.0
M29_4 6.8dB	0	10.7	100	10	150	-9583.1	309.0	-10136.6	292.6
	1					-9666.2	379.7	-10403.1	321.8
	2					-10310.6	588.8	-10976.6	473.8
	6					-14885.1	774.5	-15864.2	873.1
	7					-11092.5	484.5	-12010.5	546.0
M22_4 6.8dB noise	0	0	0	0	0	-9813.8	374.1	-10517.4	447.5
	1					-10052.4	505.6	-10641.2	451.0
	2					-10674.9	176.6	-11366.3	183.9
	6					-15125.1	764.2	-16356.7	847.3
	7					-10868.1	150.4	-11858.8	63.5

Fig. 21a shows a selected fragment of the signal registered CH0 channel within K6 configuration, and one can see the three local maxima within the averaged STFT spectrogram of this signal (Fig. 21b) giving the periodicity of AE events. It is a characteristic picture of PD related to the test voltage period [7].

The phase-time characteristics of the signal registered within K6 configuration for six measurement channel are presented in Figs 22-24. The phase-time characteristics show the periodic character of PD, which is revealed by the peaks of the tested quantity, twice during the averaged period of the supply voltage only for the CH0, CH1, CH2 and CH4 channels, whereas AE descriptors for signals registered in all channels confirm the presence of PD.

a)

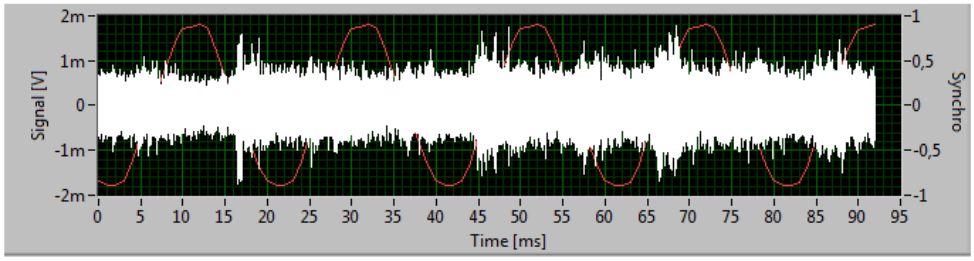

b)

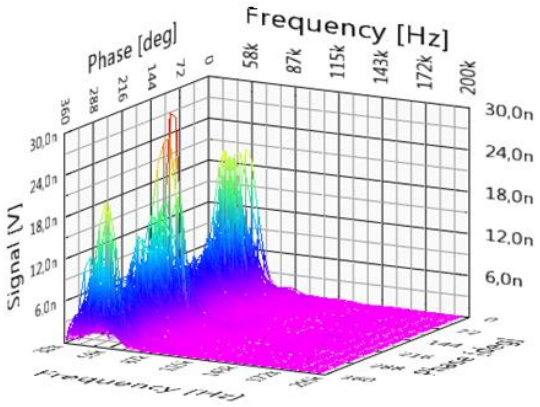

Fig. 21. AE signal recorded in the K6 configuration for the M23_46.8dB set in the CH0 measurement channel: a) the signal after filtration in the 30 kHz - 200 kHz band, b) averaged STFT spectrogram of the signal from Fig. 21a

Rys. 21. Sygnał AE zarejestrowany w konfiguracji K6 dla zestawu M23_46.8dB w torze pomiarowym CH0: a) sygnał po filtracji w paśmie 30 kHz - 200 kHz, b) uśredniony spektrogram STFT sygnału z rys. 21a

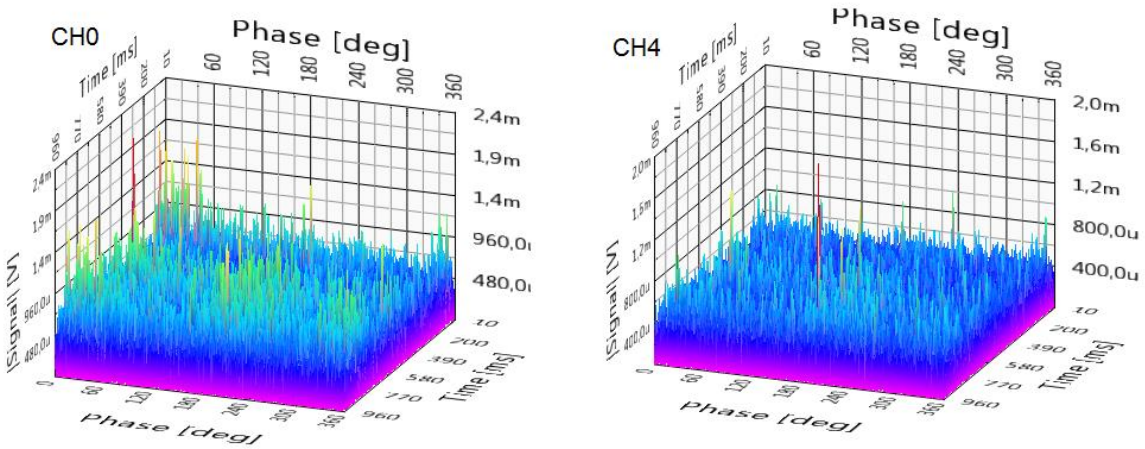

Fig. 22. Phase - time characteristics of signals recorded in measurement channels CH0 and CH4 in the following measurement situation: configuration K6, set M23_46.8dB, 400 pC, 19.8 kV

Rys. 22. Charakterystyki fazowo-czasowe sygnałów zarejestrowanych w torach CH0 i CH4 w następującej sytuacji pomiarowej: konfiguracja K6, zestaw M23_46,8dB, 400 pC, 19,8 kV

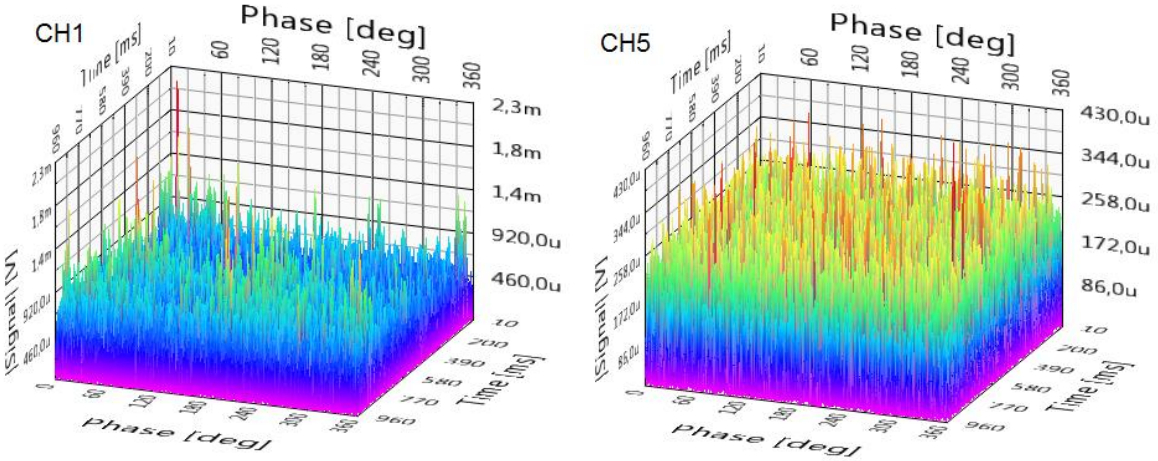

Fig. 23. Phase - time characteristics of signals recorded in measurement channels CH1 and CH5 in the following measurement situation: configuration K6, set M23_46.8dB, 400 pC, 19.8 kV

Rys. 23. Charakterystyki fazowo-czasowe sygnałów zarejestrowanych w torach CH1 i CH5 w następującej sytuacji pomiarowej: konfiguracja K6, zestaw M23_46,8dB, 400 pC, 19,8 kV

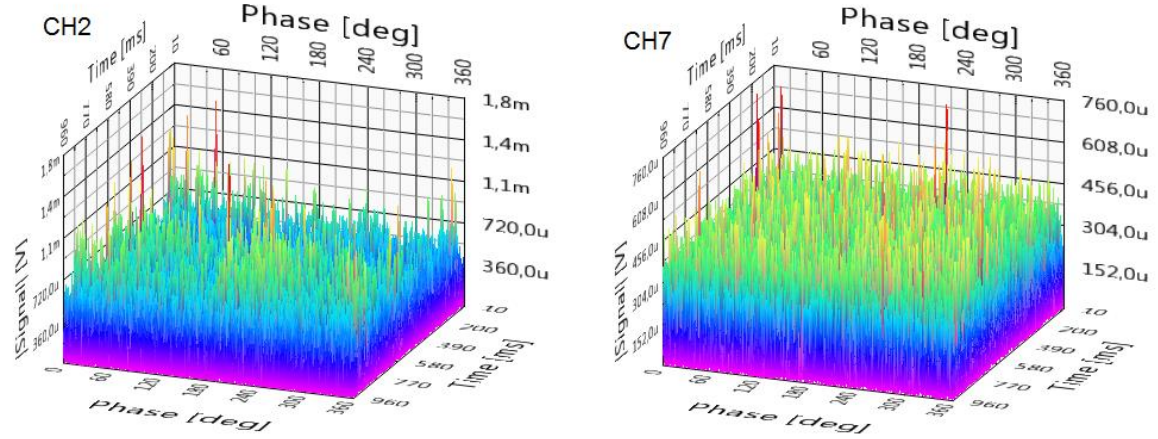

Fig. 24. Phase - time characteristics of signals recorded in measurement channels CH2 and CH7 in the following measurement situation: configuration K6, set M23_46.8dB, 400 pC, 19.8 kV

Rys. 24. Charakterystyki fazowo-czasowe sygnałów zarejestrowanych w torach CH2 i CH7 w następującej sytuacji pomiarowej: konfiguracja K6, zestaw M23_46,8dB, 400 pC, 19,8 kV

18.4. Summary

The presented test results, supported by appropriate drawings and analyzes, confirm changes in the properties of AE signals, depending on the value of the applied supply voltage and the location of the measurement points (Fig. 10). The occurrence of these changes means that the adopted research methodology allows for the analysis of deformation processes

occurring in objects and the location of PD sources. In a situation where periodic phenomena that confirm the presence of PD are not visible, the analysis conducted with the use of ADP and ADC descriptors allows to determine whether we are dealing with signals from partial discharges. The use of the descriptor method improves the process of identifying AE signals from PD. The obtained results confirm the high sensitivity of the 8AE-PD measuring system and its usefulness in PD testing in power transformers.

Bibliography

1. Duda D., Maźniewski K., Szadkowski M.: The complementary use of methods of electric and acoustic to analyze the modeled sources of partial discharges [in Polish], Przegląd Elektrotechniczny 90(10), 2014, 129–132.
2. EN 13477-2:2010 Non-destructive testing – Acoustic emission – Equipment characterisation – Part 2: Verification of operating characteristic.
3. Gacek Z., Szadkowski M., Malitowski G., Witos F., Olszewska A.: Anusual application of partial discharges to diagnose of high voltage Power transformers, Acta Phys. Pol. A 120(4), 2011, 609–615.
4. Skubis J.: Acoustic emission studies of insulation of electrical power devices [in Polish], IPPT PAN, Warszawa 1993.
5. Szerszeń G.: Low-noise preamplifier designed to work with the 8EA-WNZ computer measuring system, [in Polish], Zesz.Nauk. Pol. Śl. s. Elektryka 2014 nr 2-3, 145-158.
6. Witos F., Gacek Z.: Application of the joint electro-acoustic method for partial discharge investigations within a power transformer, European Physical Journal: Special Topics 154(1), 2008, 239–247.
7. Witos F., Olszewska A., Szerszen G.: Analysis of properties characteristic for acoustic emission signals recorded on-line in power oil transformers, Acta Phys. Pol. A 120(4), 2011, 759–762.
8. Witos F., Szerszeń G., Setkiewicz M.: Holding assembly, expecially for AE sensors to side surface of oil power transformers, 2016, Patent: PL 223 606.
9. Witos F., Szerszeń G., Opilski Z., Setkiewicz M., Olszewska A., Duda A., Maźniewski K., Szadkowski M.: Calibration and laboratory testing of computer measuring system 8AE-PD dedicated for analysis of acoustic emission signals generated by partial discharges within oil power transformers," Archives of Acoustic 42(2), 2017, 297-311.
10. Witos F., Opilski Z., Szerszeń G., Setkiewicz M.: The 8AE-PD computer measurement system for registration and analysis of acoustic emission signals generated by partial discharges in oil power transformer, Metrology and Measurements Systems 26(2), 2019, 403-418.